Conformity Rate Estimation for Shaft-Hole Pattern Fit Not Compliant with the Boundary Condition Design Criterion

Mattia Maltauro[1[0000-0002-8339-9306]], Roberto Meneghello[1[0000-0002-8099-9795]], and Gianmaria Concheri[2[0000-0001-5612-5943]].

[1] Department of Management and Engineering, University of Padova, Stradella San Nicola 3, 36100 Vicenza Italy
[2] Department of Civil, Environmental and Architectural Engineering, Laboratory of Design Methods and Tools in Industrial Engineering, University of Padova, Via Venezia 1, 35131 Padova Italy
mattia.maltauro@phd.unipd.it

Abstract. Shaft-hole pattern fits based on the Boundary Condition design criterion allows a 100% acceptability rate, but they may be not economically convenient. If the rejection rate needs to be statistically quantified and the pattern is itself the alignment feature, therefore promoted as datum feature (Intrinsic datum system), there is no trivial solution to create a tolerance stack-up: a unique assembly function cannot be determined. The focus of this contribution is "2x" patterns: different methodologies to create tolerance stack-up assessing assemblability are discussed and verified through Monte Carlo simulation. An equation to transform the variability seen from the Intrinsic datum system to the one seen from an external arbitrary reference system is given. The mutual distance between any two elements of an "nx" pattern is discussed and the implication of multiplicity and datum system is highlighted. A case, derived from an industrial case study, will be discussed by comparing the result from the simulated manual and automated assembly. A path towards "nx" patterns generalization is also presented.

Keywords: Tolerancing, Boundary Condition, Virtual Condition, Tolerance Analysis, Rejection Rate.

1 Introduction

Shaft-hole pattern fits are widely used in mechanical assemblies. They can be used for many different purposes such as bolting of plates or flanges, accurate alignment with dowel pins, etc. The Boundary Condition design criterion is a simple tool, used in the design phase, for assigning the tolerance zones that satisfy the worst-case, therefore allowing a 100% acceptability rate; the method is described in appendix B "Formulas for positional tolerancing" of ASME Y14.5-2018 [1]. Throughout this contribution, the Boundary Condition is given by the collective effect of the Feature of Size (FoS) at its

Maximum Material Size (MMS) and the location tolerance; its value shall be used to determine clearance between parts and/or to determine gage sizes [1].

The Worst Case is unlikely to occur if the Cp is equal to or greater than one. Therefore, tolerance allocation based on the statistical approach may be convenient from an economical point of view. Another reason to deviate from the Boundary Condition design criterion is that using the Worst Case approach a certain clearance is very likely to be present. Wobbling and/or vibrations may occur during operations, therefore decreasing the perceived quality by the customer [2]. For these reasons, it may be required to choose a tighter nominal fit regardless of location and size tolerances.

In all these cases, the result is a fit that does not comply with the Boundary Condition design criterion, implying a certain amount of scraps: the acceptability rate, or other metrics, must therefore be statistically quantified.

When the Maximum Material Requirement (MMR) or Least Material Requirement (LMR) [3–5] modifier is used in the geometric specification of the pattern, the possible establishment of a relationship between location and size tolerances for each FoS adds further complexity but gives, as an advantage, the reduction of non-conformal, but still functional, parts [6].

When a pattern of fits is located with reference to an External datum system (see Fig. 1.a), that functionally guarantees the alignment of the mating parts, the assembly equation is trivial and a tolerance stack-up analysis to compute the statistical metrics for each fit of the pattern can be performed. Indeed, each fit is independent of one another. Fischer [7] presents a simple mono-dimensional model to perform a tolerance stack-up that can be used also in case of material requirements (MMR or LMR). Commercial CAT (Computer Aided Tolerancing) software, e.g., CETOL 6σ™, 3DCS™, etc, can be used when the material requirement is applied to a FoS.

However, when the pattern is the datum feature, that is when the pattern is itself the alignment geometry (see Fig. 1.b), each feature is located with respect to the best fit of the pattern, which can be considered as the centroid of the actual pattern. Therefore, the actual contacts depend on the actual geometry of both mating parts. Consequently, it is not possible to know in advance in which of the single fits the contact will occur. Multiple assembly configurations are possible, and different assembly functions should be studied. The creation of a tolerance stack-up and the quantification of statistical metrics is not trivial since a unique, explicit, or implicit, assembly function is not definable.

Scholz [8], discusses the riveting problem where two holes need to match, and a pin needs to enter both holes simultaneously (floating fastener). By assuming negligible hole and pin size variability, and true position part alignment, he shows that the position mismatch increases on the order of $\sqrt{\log(n)}$. Considering "true alignment" in fact coincide with adopting an external datum system. Scholz states that the relative adjustment between the parts, that arise when the "best alignment" is considered, adds "dependency complications".

1.1 Aim of the paper

The present contribution focuses primarily on the "2x" pattern, assessing different possible methodologies that can be applied to create a tolerance analysis when the pattern

of FoS is itself the alignment feature (i.e., datum feature). The differences and implications of the two different datum systems will be discussed and a general procedure to express the variability seen from the centroid in an external arbitrary cartesian reference frame will be presented.

An analytical procedure to estimate the rejection rate, based on Root Sum of Squares (RSS) tolerance analysis, will be developed and presented. The procedure will be compared to Monte Carlo Simulation. A path towards generalization to "nx" pattern will also be discussed.

Finally, a case derived from an actual industrial study case will be presented and discussed: a pattern of two shaft-hole fits. The holes are punched into sheet metal; the shafts protrude from a plastic injection moulded part. In the assembly, the alignment is given by the fit itself. Two configurations will be studied: one assuming a manual assembly (Intrinsic datum), the second considering an automated assembly, and therefore the location tolerances given by the robotic arm (External datum).

It is noteworthy to highlight that the proposed method is relevant in the (functional) design phase: it gives the designer the possibility to simulate the impact of his design intent regardless of subsequent manufacturing decisions.

2 Materials and methods

2.1 The updated linear stack-up model

The model presented by Fischer [7], implemented in Excel, is used as a starting point for tolerance stack-ups. Several add-ons have been implemented to the model to increase efficiency and flexibility; an integrated graphical representation of the result has also been developed. The updated worksheet internally computes a new nominal value and symmetric tolerance limits when asymmetric limits are assigned. It also allows to explicitly assign, in each row, the coverage factor k, used to convert the tolerance limit in terms of standard deviation.

The worksheet has been modified to integrate the possibility to set the sensitivity coefficient ($|s|$) using an adaptation of the formulas described by Cox [9, 10].

The output mean and variance are found with the following equations:

$$\mu_{OUT} = \sum_{i=1}^{n} |s_i| \cdot \mu_i \tag{1}$$

$$\sigma_{OUT}^2 = \sum_{i=1}^{n} (|s_i|)^2 \cdot \sigma_i^2 \tag{2}$$

It must be noted that for the computation of the mean of the output (μ_{OUT}), each input mean (μ_i) should be used with their positive or negative value according to the convention found in [7], allowing considering the absolute value of the sensitivity.
Once the output mean and variance is known, the rejection rate can be easily found by integrating the Gaussian probability density function:

$$r = \int_{-\infty}^{LSL} \frac{1}{\sqrt{2\pi\sigma_{OUT}^2}} \exp\left\{-0.5\,\frac{(x-\mu_{OUT})^2}{\sigma_{OUT}^2}\right\} \partial x + \int_{USL}^{+\infty} \frac{1}{\sqrt{2\pi\sigma_{OUT}^2}} \exp\left\{-0.5\,\frac{(x-\mu_{OUT})^2}{\sigma_{OUT}^2}\right\} \partial x \tag{3}$$

Where LSL and USL are the lower and upper specification limits respectively.

2.2 General Hypothesis

The general hypotheses that are used throughout the entire work are the following:

- tol_{pos} refers to the location tolerance: the associated bilateral tolerance is half its value ($\pm tol_{\text{pos}}/2$).
- The coverage factor *k* is assumed equal to 3 for all input variables, i.e., $\sigma = \frac{tol}{3}$.
- The location variability is known from the datum system used in the specification.
- All the sizes are non-correlated.
- Feature locations are non-correlated if seen from an External datum system; correlated if seen from the Intrinsic datum system.

3 External vs Intrinsic datum system

When the pattern of FoS is located with reference to an external, and independent, completely defined, datum system, see Fig. 1.a, regardless of the multiplicity, each element is not correlated to the others. As such the actual location of each element doesn't imply any limitation in the position of the others: the covariance is null and the variance is the same for each element.

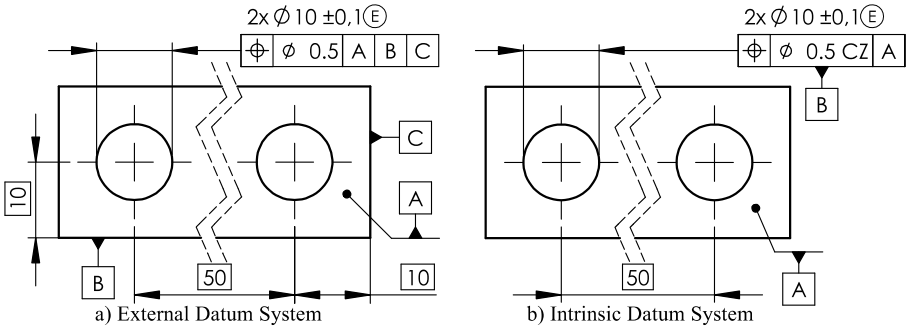

Fig. 1. Different geometric specifications for a spacer with two holes: a) External Datum System; b) Intrinsic Datum System.

In case of a pattern with multiple features, considering the $i\text{-}th$ and the $j\text{-}th$ elements, the mutual distance variance (${\sigma_L}^2$) can be expressed as follow.

$$ {\sigma_L}^2 = \text{var}(L) = \text{var}(x_j - x_i) = {\sigma_j}^2 + {\sigma_i}^2 - 2\sigma_{ij} = 2\sigma^2 \tag{4} $$

Regardless of pattern multiplicity, the actual mutual distance between any two axes (i.e., derived feature) of the fits, from a statistical point of view, can therefore be written as:

$$ \text{L} = \text{L}_{\text{nom}} \pm \sqrt{2} \cdot \frac{\text{tol}_{\text{pos}}}{2} \tag{5} $$

When the pattern is specified with the CZ indication and is promoted as a datum feature, see Fig. 1.b, the datum system origin can be assumed as the centroid of the pattern. In this reference system, the centroid is fixed, as such $x_G = 0$ and $\sigma_G = 0$.

For a "nx" pattern the centroid variance can be expressed as follow:

$$\sigma_G{}^2 = 0 = \sum_{i=1}^{n} \frac{\sigma_i{}^2}{n} + \frac{2}{n} \sum_{i>j} \sigma_{ij} \tag{6}$$

From the last equation, assuming the same variance for all the pattern elements and the same covariance for each pair of elements, the covariance can be found:

$$\sigma_{ij} = -\frac{1}{n-1} \sigma_i{}^2 \tag{7}$$

Using this result, the variance for the mutual distance of any pair of a "nx" linear pattern can be found.

$$\sigma_L{}^2 = 2 \frac{n}{n-1} \sigma_i{}^2 \tag{8}$$

It is noteworthy that for an infinite pattern the result coincides with the one found for an External datum system; this means that the covariance decreases when the number of elements increases. At the infinite limit there is no more correlation and dependency.

The mutual distance between two fits located from the centroid can be written as:

$$L = L_{\text{nom}} \pm \sqrt{2 \frac{n}{n-1}} \cdot \frac{tol_{\text{pos}}}{2} \tag{9}$$

It can be noted that the use of the Intrinsic datum system has an impact on the variability of the mutual distance between two elements of the pattern.

3.1 Datum system transformation

To perform a Monte Carlo simulation when dealing with an Intrinsic datum system, because of the dependency between the reference system and the actual pattern situation, it is not possible to directly sample the location of the pattern. It is necessary to base the sampling on an independent reference system.

If σ is the variability (expressed as standard deviation) seen from the centroid reference system and $\tilde{\sigma}$ is the variability seen from any external fixed reference system, the following relation can be found.

$$\frac{\tilde{\sigma}}{\sigma} = \sqrt{\frac{n}{n-1}} \tag{10}$$

To prove equation (10) a Monte Carlo simulation has been performed for a "2x" and a "3x" patterns. Given a fixed value for the standard deviation seen from the external reference system, 500'000 samples have been simulated. Per each sample, the pattern location from the centroid is computed and statistical metrics are found and compared to the one seen from the External datum system, see Table 1 and Table 2.

Table 1. Monte Carlo simulation results for 2x pattern.

External Reference System				Intrinsic Reference System				Comparison	
X_1		X_2		x_1		x_2			
$\bar{X}_1$	0.000	$\bar{X}_2$	80.000	$\bar{x}_1$	-40.000	$\bar{x}_2$	40.000	Theoretical $\sqrt{\frac{n}{n-1}}$	1.414
$\tilde{\sigma}_1$	0.067	$\tilde{\sigma}_2$	0.067	σ_1	0.047	σ_2	0.047	Experimental $\frac{\tilde{\sigma}}{\sigma}$	1.416

Table 2. Monte Carlo simulation results for 3x pattern.

External Reference System					Intrinsic Reference System						Comparison	
X_1		X_2		X_3	x_1		x_2		x_3			
$\bar{X}_1$	0.000	$\bar{X}_2$	80.000	$\bar{X}_3$ 160.000	$\bar{x}_1$	-80.000	$\bar{x}_2$	0.000	$\bar{x}_3$	80.000	Theoretical $\sqrt{\frac{n}{n-1}}$	1.225
$\tilde{\sigma}_1$	0.067	$\tilde{\sigma}_2$	0.067	$\tilde{\sigma}_3$ 0.067	σ_1	0.054	σ_2	0.054	σ_3	0.054	Experimental $\frac{\tilde{\sigma}}{\sigma}$	1.225

The result of the simulation confirms the transformation formula, the error is well below 1% in both cases. Skewness and Kurtosis, not displayed, both confirm that in both cases the distribution seen from the centroid tends to normality as expected.

4 2x Patterns stack-up

In this section different methodologies to create a tolerance stack up when the reference system is based on the centroid are presented. The geometric specification for the shaft can be seen in Fig. 2, the specification for the holes in Fig. 1.b. The Boundary Condition for holes is $9.9 - 0.5 = 9.4$ mm, while for shafts is $10 + 1 = 11$ mm, therefore no 100% fit is allowed, and the resulting rejection rate must be estimated.

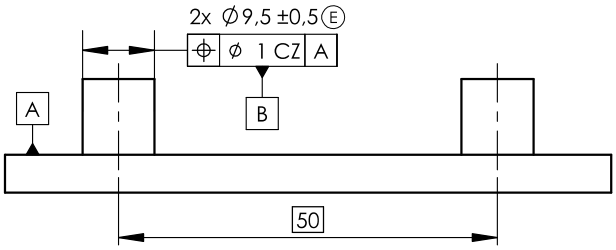

Fig. 2. Geometric specification for a two shafts cap

4.1 Stack-up by cases

For a “2x” pattern, one element can be considered as master and the gap can be evaluated on the second one. In this case, two different assembly equations can be found, and for each one, a unilateral gap can be analysed, see Fig. 3.

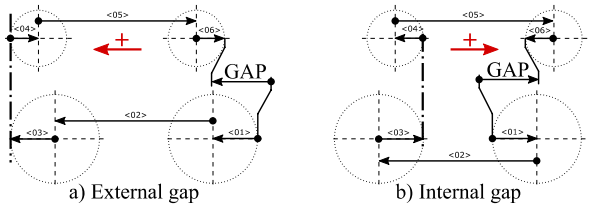

Fig. 3. Stack-up scheme

With the first case, it is possible to compute the rejection rate for overshoot, the second case gives the rejection rate for undershoot. The overall rejection rate is the sum of the two.

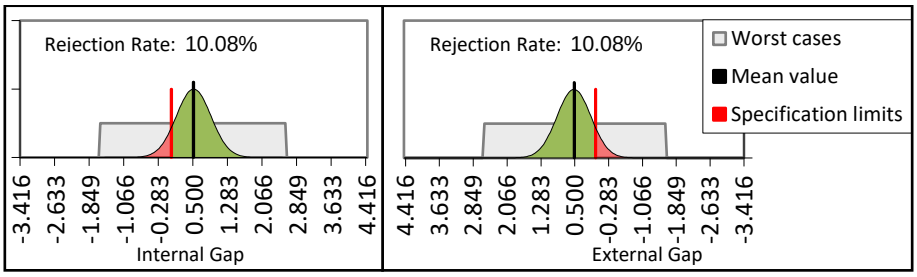

Fig. 4. External and Internal gap distribution and rejection rate, stack-up by cases

A generalized gap, able to consider both internal and external gaps simultaneously, can be defined by applying a dummy upper limit equal to twice the mean gap, the rejection rate and other statistical metrics can be directly found in the worksheet, see Fig. 5.

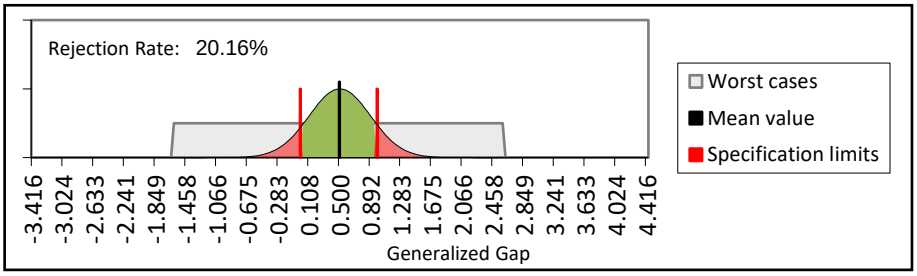

Fig. 5. Generalized Gap distribution and Rejection Rate, stack-up by cases

This method, generalized gap excluded, is a straightforward application of the model as described by Fischer [7] and, although consistent, does not use a rigorous definition of the datum system. In sections 4.2, 4.3, and 4.4 alternative methods, tested by the Authors, are proposed.

4.2 Symmetric stack-up

Considering that the pattern is symmetric with respect to the datum system, the tolerance stack-up can be centered, considering the datum systems of the mating parts aligned. Consequently, one single fit can be studied. Two distinct unilateral gaps can be defined, see Fig. 6.a).

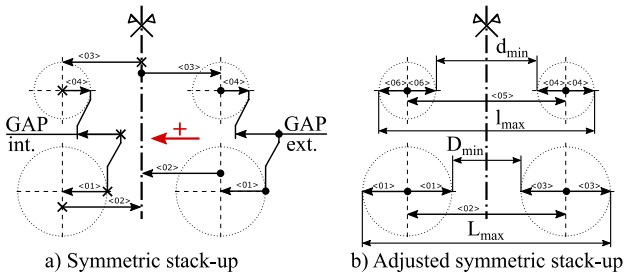

Fig. 6. Stack-up scheme for all symmetric cases: a) Internal and external gaps for the symmetric stack-up; b) Elements use in the symmetric adjusted stack-up.

As for the previous case, a generalized gap can be defined and statistical metrics computed, see Fig. 7.

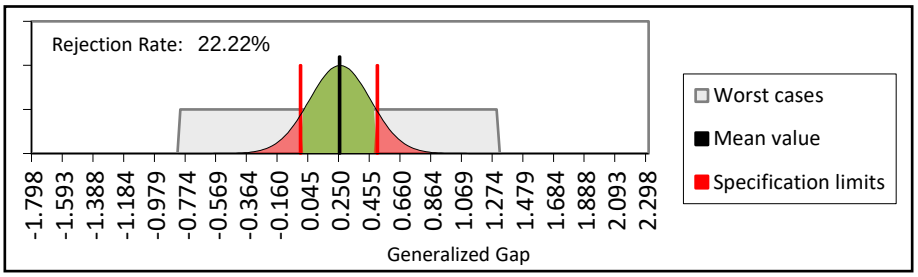

Fig. 7. Generalized Gap distribution and Rejection Rate, symmetric stack-up

The rejection rate is higher than the one found with the previous method. In this case, the true position alignment is considered and the size of the two FoS are correlated.

4.3 Symmetric adjusted stack up

To overcome the limitation highlighted in 4.2, an adjustment to the model can be implemented. Instead of studying only half of the pattern, the whole pattern is considered. The distance from the datum system of the second FoS is correlated to the first one, consequently, it cannot be added: the half distance must be duplicated instead, using a sensitivity of 2. Four gaps are now to be considered, but two by two are symmetrical. By considering the gaps given by the difference $L_{\max} - l_{\max}$ (Sum of the external gaps)

e $d_{\min} - D_{\min}$ (Sum of the internal gaps), it is possible to study, as for the previous cases, two unilateral gaps, see Fig. 6.b.

A generalized gap can also be defined by adding a dummy upper limit as in the previous cases, see Fig. 8.

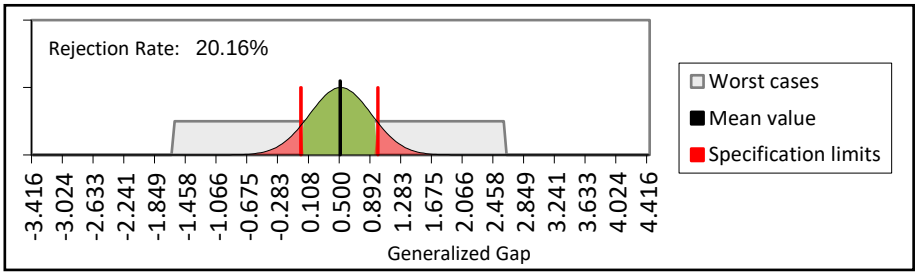

Fig. 8. Generalized Gap distribution and Rejection Rate, symmetric adjusted stack-up

In this case, the rejection rate is equal to the one found with the first method: it can represent the non-linearities due to the contact points. Moreover, since it starts from the datum system, the material condition can be added.

4.4 Symmetric optimized stack up

The model as described can be further optimized since the TED (Theoretically Exact Dimension, i.e., Nominal dimension) contribution can be neglected, it does not give any contribution to the gap, and the FoS contribution can be added once by using a sensitivity equal to 1 and scaling the tolerance of a factor $1/\sqrt{2}$ that adjust the contribution to count the independence between the two-element sizes. However, this does not allow considering the material conditions.

4.5 Monte Carlo Verification

To verify the result of the proposed method a Monte Carlo simulation is used. The standard deviation associated to the localization of the FoS is "corrected" with the relation given by equation (10), a total number of 500'000 combinations for the eight variables are initiated and both the external and internal gaps are calculated. If both gaps are positive the assembly is accepted.

The variability seen from the centroid and its normality is checked.

Over twenty re-computation of the simulation, the average rejection rate is 20.15% with a standard deviation of 0.06% against an analytical value of 20.16%.

The analytical model is therefore considered verified.

5 Path towards generalization

To generalize the proposed method to a "nx" linear pattern it is first possible to define $n-1$ independent pairs of FoS in the pattern.

For each independent pair, the method can be applied considering the location variability seen from the centroid of the pair that can be found equal to half of the variability of the mutual distance. The rejection rate (r_i) for any pair can be determined, and the probability that the assembly is successful ($P = P(i) = 1 - r_i$) as well. If each pair is considered stochastically independent $P(j|i) = P(j)\ \forall\ j, i$, the probability that both the j-th and the i-th pairs can be assembled is $P(j \cap i) = P(j)P(i) = P^2$.

It can be easily derived that for a "nx" pattern the probability to assemble the pattern, according to the given hypothesis, is $P_n = P^{n-1}$. The rejection rate accordingly becomes $r_n = 1 - [1 - r]^{n-1}$.

Through Monte Carlo simulation, this equation was not verified: the probability of assembling a further pair of the pattern is less than the previous ones since the relative adjustment between the mating FoS depends on the actual situation of the previous pairs.

A more general equation for the rejection rate is proposed:

$$r_n = 1 - [1 - \beta \cdot r]^{n-1} \tag{11}$$

Where $\beta \geq 1$ is a coefficient that needs further investigation to determine which parameters it depends on.

The formalization of the method for a "nx" pattern may be used also for rectangular and circular patterns. In the first case, a rectangular pattern (p x q = n) may be decomposed into two "nx" patterns along the two principal directions. A "nx" circular pattern may be considered as a linear "nx" pattern if a curvilinear coordinate is used.

6 The case study

The geometric specification for the case study, derived from an actual industrial case, can be seen in Fig. 9. The dimensions and tolerances have been modified ensuring the same general proportions.

Using the method proposed in section 4.3, the estimated rejection rate, under "best alignment" (manual assembly) is 24.16%.

To simulate the automated assembly, first, the model presented in section 4.2 should be used to exclude the possible adjustment between parts during assembly. As second, two additional terms should be added, the first on the sheet metal part to describe the variability between the centroid of the pattern and the alignment features used by the robotic arm (not in the specification), the second on the cap side to describe the robotic arm precision.

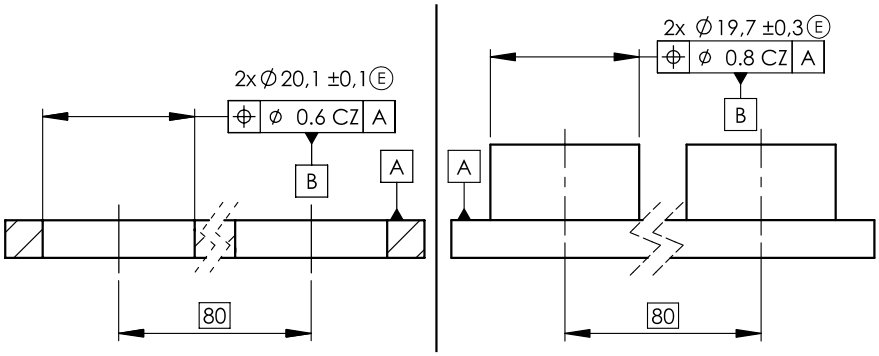

Fig. 9. Geometric specification for the case study

In the stack-up, the first term is assumed $\pm 0.3\text{mm}$, the second one $\pm 0.1\text{mm}$.

The estimated rejection rate now becomes 32.72%. The difference (8.56%) stands for a fraction of parts that cannot be assembled by the specific assembly process that has been chosen.

This value may be lowered by changing the automated assembly process considering its associated costs.

It is noteworthy to highlight that the automated assembly adds another source of uncertainty to the stack-up. The functional specification for pattern fits should describe the assemblability as a necessary requirement for the mating parts. As a result of the case study, the assemblability of the pattern fit depends on the actual assembly process. For this reason, it is important to distinguish functional and manufacturing specifications: the latter should consider each step of the production (assembly included) and eventually tighten the tolerance values. The manufacturing specification should be used to tune the process since it transforms the functional specification assigning tighter limits based on the whole manufacturing chain; the functional specification still represents the non-negotiable boundary that when exceeded does not guarantee functionality.

7 Conclusions

The aim of this contribution was to define a method to assess the rejection rate for a pattern of fits not compliant with the Boundary Condition design criterion with a particular focus on the case in which the pattern is itself the alignment feature. The 2x case was deeply investigated and a method based on RSS was proposed and verified through a Monte Carlo simulation.

If an Intrinsic datum system is used, dependency among the locations of the features arises, equation (7) can be used to find the statistical covariance.

Equation (10) has been presented and verified to perform Monte Carlo simulation when the Intrinsic datum system is used in the pattern specification.

The use of a dummy upper limit to study a single statistical bell for the two gaps that a fit create has been presented and the result was verified through Monte Carlo simulation.

A case, derived from an industrial study case, was presented and resolved: it was possible to simulate the difference between by hand and automated assembly.

Equation (11) may represent the analytical generalization to a "nx" linear pattern but further investigations are needed to fully define the β parameter; a generalization for a rectangular pattern should also be investigated.

The analytical definition of a pattern fit may be used to define a new kind of Kinematic constrain to be used in stack-up analyses. The current practice consists in defining a primary and secondary fit to define the kinematic constrain between mating parts.

It can also be used for formal computation of "nx" dowel pins where more than two pins with greater clearance behave as two tighter pins.

References

1. ASME: ASME Y14.5 - 2018 - Dimensioning and Tolerancing, New York (2019).
2. Bastiaan, J.M., Green, E., Kaye, S.: Preliminary Study of Perceived Vibration Quality for Human Hands. SAE Int. J. Adv. Curr. Pract. Mobil. 1, 1741–1754 (2019). https://doi.org/10.4271/2019-01-1522.
3. ISO International Organization for Standardization: ISO 2692:2021 - Geometrical product specifications (GPS). Geometrical tolerancing. Maximum material requirement (MMR), least material requirement (LMR) and reciprocity requirement (RPR), Geneva (2021).
4. Pierre, L., Anselmetti, B., Anwer, N.: On the usage of least material requirement for functional tolerancing. In: Procedia CIRP. pp. 179–184 (2018). https://doi.org/10.1016/j.procir.2018.04.068.
5. Anselmetti, B., Pierre, L.: Complementary Writing of Maximum and Least Material Requirements, with an Extension to Complex Surfaces. In: Procedia CIRP. pp. 220–225 (2016). https://doi.org/10.1016/j.procir.2016.02.153.
6. Markiewicz, M., Bachtiak-Radka, E., Dudzińska, S., Grochała, D.: Statistical Process Control Using LMC/MMC Modifiers and Multidimensional Control Charts. In: Hamrol A., Grabowska M., Maletic D., Woll R. (eds) Advances in Manufacturing II. MANUFACTURING 2019. Lecture Notes in Mechanical Engineering. pp. 244–253. Springer, Cham (2019). https://doi.org/10.1007/978-3-030-17269-5_18.
7. Fischer, B.R.: Mechanical Tolerance Stackup and Analysis. CRC Press (2004). https://doi.org/10.1201/9780203021194.
8. Scholz, F.: Title Hole Alignment Tolerance Stacking Issues. , Seattle (1999).
9. Cox, N.D.: Volume 11: How to perform statistical tolerance analysis. American Society for Quality Control, Milwaukee, WI (1986).
10. Cox, N.D.: Tolerance Analysis by Computer. J. Qual. Technol. 11, 80–87 (1979). https://doi.org/10.1080/00224065.1979.11980884.